Respiratory Research

RESEARCH

Open Access

Levosimendan mediates the BMP/Smad axis through upregulation of circUSP34-targeted miR-1298 to alleviate pulmonary hypertension

Qiang Meng[1], Linhong Song[1,2], Hui Wang[1], Gang Wang[1] and Gengxu Zhou[1*]

Abstract

Background Pulmonary hypertension (PH) is a long-term disease that impacts approximately 1% of the world's population. Currently, levosimendan (Lev) is proposed for PH treatment. However, the mechanism of Lev in the treatment of PH is unknown.

Methods We used hypoxia-induced pulmonary artery smooth muscle cells (PASMCs) to establish a PH cell model. A number of cell biology methods were performed to assay alterations in cell proliferation, migration and apoptosis after Lev treatment. qRT-PCR and WB were performed to test the levels of circUSP34 and miR-1298, and BMP/Smad protein respectively. In addition, the regulatory relationship between circUSP34 or BMPR2 with miR-1298 was verified through the use of double luciferase as well as RIP assay. In addition, we explored the regulatory effect of Lev on the circUSP34/miR-1298/BMP/Smad axis using a rat PH model.

Results Our results demonstrate that Lev inhibited PASMCs cell proliferation, migration and promoted apoptosis exposed to hypoxia. In hypoxia-treated PASMCs, circUSP34 expression got downregulated while miR-1298 upregulated, whereas the addition with Lev resulted in upregulation of circUSP34 expression and downregulation of miR-1298 expression, indicating that circUSP34 can target and regulate miR-1298. In addition, miR-1298 targets and regulates the expression of BMPR2. In a rat PH model induced by hypoxia combined with SU5416, Lev upregulated circUSP34 targeting miR-1298-mediated BMP/Smad axis to alleviate the PH phenotype.

Conclusion We have shown that Lev can be used as a therapeutic drug for PH patients, which works through the circUSP34/miR-1298/BMP/Smad axis to alleviate PH symptoms.

Keywords Pulmonary hypertension, Levosimendan, CircUSP34, MiR-1298, BMP/Smad axis

*Correspondence:
Gengxu Zhou
zhougengxu0016@163.com
[1]Department of Pediatric Cardiac Surgery, The Seventh Medical Center of the PLA General Hospital, Beijing 10010, P.R. China
[2]The Second School of Clinical Medicine, Southern Medical University, Guangzhou, Guangdong Province 510515, P.R. China

Introduction

Pulmonary hypertension (PH) is the definition of a mean pressure in the pulmonary arteries that exceeds 20 mm Hg. PH can lead to poor heart function and may cause fatigue, shortness of breath on exertion, swelling in the legs or abdomen, chest pain, and dizziness or fainting [1, 2]. PH is classified in five main classes: PH caused by rupture or stenosis of the pulmonary arteries; PH due to heart disease; PH resulting from lung disease; PH resulting from blockage of blood vessels; and PH caused by other causes [3]. PH is a long-term disease that impacts approximately 1% of the world's population [4]. Studies have shown that the pathophysiological changes of PH are pulmonary vasoconstriction and pulmonary vascular remodeling, among them, the abnormal multiplication of pulmonary vascular cells plays pivotal role in the development of PH [3]. Currently, drug therapy can provide clinical improvement in patients with PH, but it cannot reverse the process of pulmonary vascular remodeling and prevent of PH progression [4, 5]. Hence, an in-depth understanding of the pathogenic mechanisms of PH and the development of effective drugs are urgently needed.

Circular RNA (circRNA) is non-coding RNA is generated from linear pre-mRNAs in a non-classical patchwork way, which gives them a distinctive closed sequential loop structure that is less susceptible to degradation by nucleases [6, 7]. CircRNAs have these characteristics that suggest that they have different potential biological functions and are relevant to the occurrence of many human diseases [8]. Recently, there is growing evidence that circRNAs are considered to be essential modulators in the developing PH [9]. Aberrant expression in circRNAs with their targets has a key function in lung vascular remodelling and PH [10]. As recently shown circSirt1 suppressed TGF-β1/Smad3/Smad7-mediated PH by regulating SIRT1 mRNA expression [11]. Low expression of circSMOC1 promoted metabolic reprogramming through PTBP1 and miR-329-3p in rats with PH [12]. Moreover, studies previously conducted have shown that the expression of the novel circUSP34 is dysregulated in chronic thromboembolic PH [13], suggesting that circUSP34 may be involved in PH progression. Nevertheless, the regulatory mechanism of circUSP34 in PH is unclear.

MicroRNAs (miRNAs) are minor non-coding RNAs (21–23 nucleotides) that modulate post-transcriptional levels of genes and play key roles in a variety of critical biological processes [14]. An increasing body of evidence has indicated the involvement of miRNAs in the progression of PH [15]. For example, miR-21 levels correlate with the severe degree of right ventricular dysfunction in patients with PH [16]. MiR-150 protects against pulmonary vascular remodeling and fibrosis during hyperoxia-induced PH [17]. A recent study has shown that miR-1298 was upregulated in the right ventricle of PH rats compared with normal rats [18]. A growing amount of evidence indicates that circRNAs are participated in the development of many diseases through mechanisms related to their role as sponge-adsorbing miRNAs [19, 20]. The StarBase database predicts a presumptive binding site as between miR-1298 with circUSP34. However, whether miR-1298 is associated with circUSP34 in PH remains to be investigated.

Levosimendan (Lev) is a calcium-sensitizing agent with positive inotropic effects in acute decompensated chronic heart failure [21]. Currently, Lev has been brought into the clinical practice for the therapy of right ventricular failure [22], which displays positive inotropic effects by sensitizing cardiac troponin C to calcium [23]. Lev is also an effective vasodilator by turning on the action of adenosine triphosphate-sensitive potassium channels (KATP) [24]. Therefore, it has also been suggested for PH treatment [25, 26]. However, the therapeutic effects and mechanism of Lev in the treatment of PH remain unclear.

In this study, we have found that Lev inhibits cell proliferation, migration and promotes apoptosis among hypoxia-treated pulmonary artery smooth muscle cells (PASMCs). CircUSP34 expression was downregulated and miR-1298 expression was upregulated in hypoxia-treated PASMCs. When treated with Lev, circUSP34 expression was upregulated, whereas miR-1298 expression was downregulated, indicating that circUSP34 could target and regulate miR-1298. In addition, miR-1298 targeted and regulated BMPR2 expression to affect cell proliferation, migration and apoptosis in hypoxia-treated PASMCs. In PH rat model using hypoxia combined with SU5416-induced, Lev upregulated circUSP34 targeting miR-1298-mediated BMP/Smad axis to alleviate the PH phenotype.

Methods

Cell culture

Human PASMCs (Catalog No. 3110) that were acquired at ScienCell where they were grown in smooth muscle cell culture medium (SMCM, ScienCell) at 37 °C in a humidified normoxia condition (21% O_2, 5% CO_2, 74% N_2) for passaging. Hypoxia (3% O_2, 5% CO_2, 92% N_2) was achieved by injecting nitrogen into the incubator, and the oxygen concentration in the chamber was continuously monitored with an oxygen sensor. For Lev (Orion Pharma, Finland)-treated cell experiments, PASMCs were continued for 24 h under hypoxic conditions after the addition of Lev (final concentration of 1 μM, 10 μM).

Plasmid construction and cell transfection

Sequences of the shRNA for circUSP34 and BMPR2 knockdown were cloned into the PLKO vector. Empty PLKO vectors were employed as negative control (sh-NC). PASMCs were transfected by using Lipofectamine™

2000 (Invitrogen, USA) with the corresponding constructs according to the manufacturer's directions. MiR-1298 mimic or miR-1298 inhibitor had been purchased from GenePharma (Shanghai, China). When cells were grown to about 80% of confluence, miR-1298 mimic or miR-1298 inhibitor had been transfected into PASMCs, separately.

Cell counting Kit-8 (CCK-8) assay

CCK-8 was obtained from Abcam. Cell viability measurements have been conducted based on the manufacturer's directions provided. Briefly, PASMCs were cultured in 96-well plates for 12 h. 10 μL of CCK-8 reagent and 90 μL of medium were added in each well and cells were incubated at 37 °C for 30 min. The light density values were measured at 450 nm.

Immunofluorescence (IF) assay

PASMCs were seeded onto slides into 6-well plates and grown on the slides. Cells then were fixated, permeabilized, and stained with anti-Ki-67 (Abcam, ab15580) and DAPI (Cell Signal Technology, 4083). Images were obtained with an Olympus confocal microscope FV3000 (Olympus, Japan).

Scratch assay

PASMCs were grown on 6-well culture plates until they reached 80% confluence after 24 h. The layers of cells were scratched into a single line with a 1 mL pipette tip. After that, the cell monolayer was gently washed to remove the detached cells, then supplemented with fresh medium and the created wound was imaged with a phase contrast microscope (Olympus, Japan). Images were captured with phase contrast microscope 24 h later to observe cell migration.

Flow Cytometry

Apoptosis rate of PASMCs was tested by Annexin V-FITC/PI Apoptosis Assay Kit (Vazyme, China). Firstly, 1×10^5 cells were seeded in 6-well plates and incubated for 24 h. After treatment and continuous culture for 24 h, cells were labeled with 5 mL Annexin V-FITC and PI for 20 min in the dark at room temperature. Afterwards, cells were assayed and examined on a BD LSRFortessa flow cytometer (BD, USA). Flowjo (BD, USA) was employed to quantitatively determine the percentage of apoptotic cells.

Quantitative real-time PCR (qRT-PCR)

Total RNA was isolated from PASMCs and rat lung tissue with Trizol kit (Thermo Scientific, USA), followed by first-strand cDNA synthesis with a high-capacity RNA-to-cDNA kit (Thermo Scientific, USA). The fluorescence intensity of real-time PCR reactions was monitored with the Power-SYBR Green PCR Master Mix (Thermo Scientific, USA) by placing ABI QuantStudio 5 (Thermo Scientific, USA) system. Relative expression of genes was calculated by the $2^{-\Delta\Delta CT}$ method, using β-actin or U6 as reference genes. Corresponding primers are indicated as follows: circUSP34, F: 5'-GCC AAA GAA AGA AAA ACT AAA GTG G-3' and R: 5'-AGG TCT CAG CCT CTG AAT CAC-3'; BMPR2, F: 5'-GAC AGG AGA CCG TAA ACA AGG-3' and R: 5'-CCA TAT CGA CCT CGG CCA ATC-3'; β-actin, F: 5'-TGG CAC CAC ACC TTC TAC AA-3' and R: 5'-CCA GAG GCG TAC AGG GAT AG-3'; miR-1298, F: 5'-TCA TTC GGC TGT CCA GA-3' and R: 5'-GAA CAT GTC TGC GTA TCT C-3'; U6, F: 5'-CTC GCT TCG GCA GCA CA-3' and R: 5'-AAC GCT TCA CGA ATT TGC GT-3'.

Western blot (WB)

PASMCs and lung tissue of rats were lysed using RIPA buffer and protein quantification in obtained lysates was performed by the BCA method. Sodium dodecyl sulfate-polyacrylamide gel electrophoresis (SDS-PAGE) was performed to separate proteins, which then the cut gels were transferred to polyvinylidene fluoride (PVDF) membranes. After blocking with 5% skim milk for 1 h, the membranes were kept at 4 °C and incubated overnight with the following primary antibodies: BMPR2 (1:1000, Abcam, ab130206), BMP4 (1:1000, Cell Signaling Technology, 4680), Smad1/5/8 (1:1000, Abcam, ab13723), p-Smad1/5/8 (1:1000, Sigma-Aldrich, AB3848-I), Id1 (1:1000, Abcam, ab168256), β-actin (1:2000, Cell Signaling Technology, 4967). After washing with Tris-buffered saline containing Tween (TBST), the membranes were incubated with the corresponding secondary antibody (1:5000, Cell Signaling Technology, 7074) for 2 h at 37 °C. Protein signals were detected on a Tanon 5200 series fully automated chemiluminescence analysis system (Tanon, China) using enhanced chemiluminescence reagents (Vazyme, China). The band intensity was quantified with the use of ImageJ.

RNA immunoprecipitation (RIP)

PASMCs were lysed with the Magna RIP™ RNA Binding Protein Immunoprecipitation Kit (Millipore, USA). The magnetic beads were conjugated to anti-AGO2 and anti-IgG and were incubated at 4 °C overnight with the cell lysate. Lastly, the total RNA was separated and purified with TRIzol reagent (Thermo Scientific, USA) and controlled by qRT-PCR analysis.

Dual luciferase assay

The luciferase reporter vectors circUSP34-WT (BMPR2-WT) and circUSP34-MUT (BMPR2-MUT) were synthesized by GenePharma (Shanghai, China). The binding site sequences of circUSP34 (circUSP34-WT/MUT) or

BMPR2 (BMPR2-WT/MUT) were introduced into pSI-check2 vectors (Promega, Madison, WI), respectively. The miR-1298 mimic and mimic NC were then transfected into PASMCs by Lipofectamine™ 2000. After 48 h of transfection, the luciferase activity was assayed with a dual luciferase reporter system (Promega, USA) following manufacturer's directions.

PH rat model construction

Twenty-four male SD (Sprague-Dawley) rats (weighing 180–220 g) were brought from Nantong Trophic Feed Technology Co. All rats were reared under pathogen-free conditions and divided randomly into four groups: Control group, PH model group, PH+3 mg/kg Lev and PH+30 mg/kg Lev ($n=6$). Lev was given at 3 mg/kg/d or 30 mg/kg/d in drinking water to maintain the target dose of oral Lev, which was adjusted twice a week according to the amount of water consumed. A rat model of PH was established by using hypoxia combined with SU5416 treatment. In the SU5416/hypoxia model, rats were subcutaneously injected with SU5416 (20 mg/kg), the vascular endothelial growth factor KDR receptor inhibitor, once a week and placed in hypoxia (10% O_2) for 3 weeks. Control rats were given the equivalent volume of drug alone and kept at 21% O_2 in the same room adjacent to the hypoxic chamber. Following 3 weeks of hypoxia and a series of weekly administrations of Lev, the rats have been administered anesthesia with ethyl carbamate (1 g/kg) and sacrificed with cervical dislocation. Then, pulmonary artery tissue was collected. All animal study protocols were authorized by the Animal Ethics Committee of the Seventh Medical Center of the PLA General Hospital.

Hemodynamic and ventricular hypertrophy analysis

The rats were evaluated for mean pulmonary artery pressure (mPAP) after the experiment. Rats were anesthetized with urethane. A heparinized pressure volume (PV)-1 catheter was brought in to the pulmonary artery through the extra-jugular vein, right atrium as well as the right ventricle, and mPAP was tested. The hearts were harvested from the PH rat and weighed. The ratio of right ventricular (RV) to left ventricular (LV) plus the interventricular septum (IVS) (RV/[LV+IVS]), which is the right heart hypertrophy index (RVI), was then calculated. Following anesthesia, the rats were connected to a topical ventilator for mechanical ventilation, after which the mean RV systolic pressure (RVSP) and LV systolic pressure (LVSP) (in mmHg) were recorded over 10 stable heartbeats using PowerLab monitoring hardware and software (ADInstruments).

Hematoxylin-eosin (HE) and masson staining

PH rat pulmonary tissue samples were formalin-fixed, paraffin-embedded and sectioned, followed by HE and Masson staining. All images were taken with an Olympus microscope (Olympus, Japan).

Immunohistochemical (IHC) assay

Sections of PH rat pulmonary artery tissue samples were formalin-fixed, paraffin-embedded, and pathologically confirmed. The tissue sections were stained immunohistochemically with anti-Ki-67 antibodies and avidin-biotin peroxide with 3,3′-diaminobenzidine. All images were acquired by an Olympus microscope (Olympus, Japan).

Terminal deoxynucleotidyl transferase dUTP nick end labeling (TUNEL) staining

PH rat pulmonary artery tissue samples were formalin-fixed, paraffin-embedded and sectioned, labelling was then performed following the protocol of the TUNEL BrightRed Apoptosis Detection Kit (Vazyme). Characterization of apoptotic cells by TUNEL assay. Images were acquired via an Olympus microscope (Olympus, Japan) and the TUNEL positive cell ratio was then calculated.

Statistical analysis

Data are reported as mean±SD for at least three distinct studies. Student's *t*-test was employed to identify any differences between the two groups. One-way ANOVA was used to compare differences between various groups. $P<0.05$ was considered statistically significant.

Results

Lev suppresses cell proliferation, migration and promotes apoptosis in hypoxia-treated PASMCs

To study the role of Lev in PH, we treated PASMCs with hypoxia to develop a cellular model of PH. The cell proliferation ability of PASMCs was assayed by CCK-8, and the results showed that hypoxia significantly promoted cell proliferation compared with normoxia treatment (Fig. 1A). The expression of Ki-67 was measured by IF, and it was revealed that hypoxia treatment dramatically increased the Ki-67 protein expression level (Fig. 1B). Scratch assay examined the cell migration ability of PASMCs and revealed that hypoxia significantly promoted cell migration compared with normoxia treatment (Fig. 1C). Flow cytometry was performed to investigate the effect of hypoxia on PASMCs apoptosis and showed that hypoxia markedly reduced apoptosis compared with normoxia treatment (Fig. 1D). In addition, we treated the hypoxia-induced PASMCs with 1 μM and 10 μM Lev to assess the proliferation, migration and apoptosis of PASMCs. The results indicated that the higher Lev concentration applied treatment markedly inhibited cell proliferation and decreased Ki-67 protein expression (Fig. 1A and B). Apart from that, high Lev treatment also greatly reduced cell migration and facilitated cell apoptosis (Fig. 1C and D). Previous studies have identified that

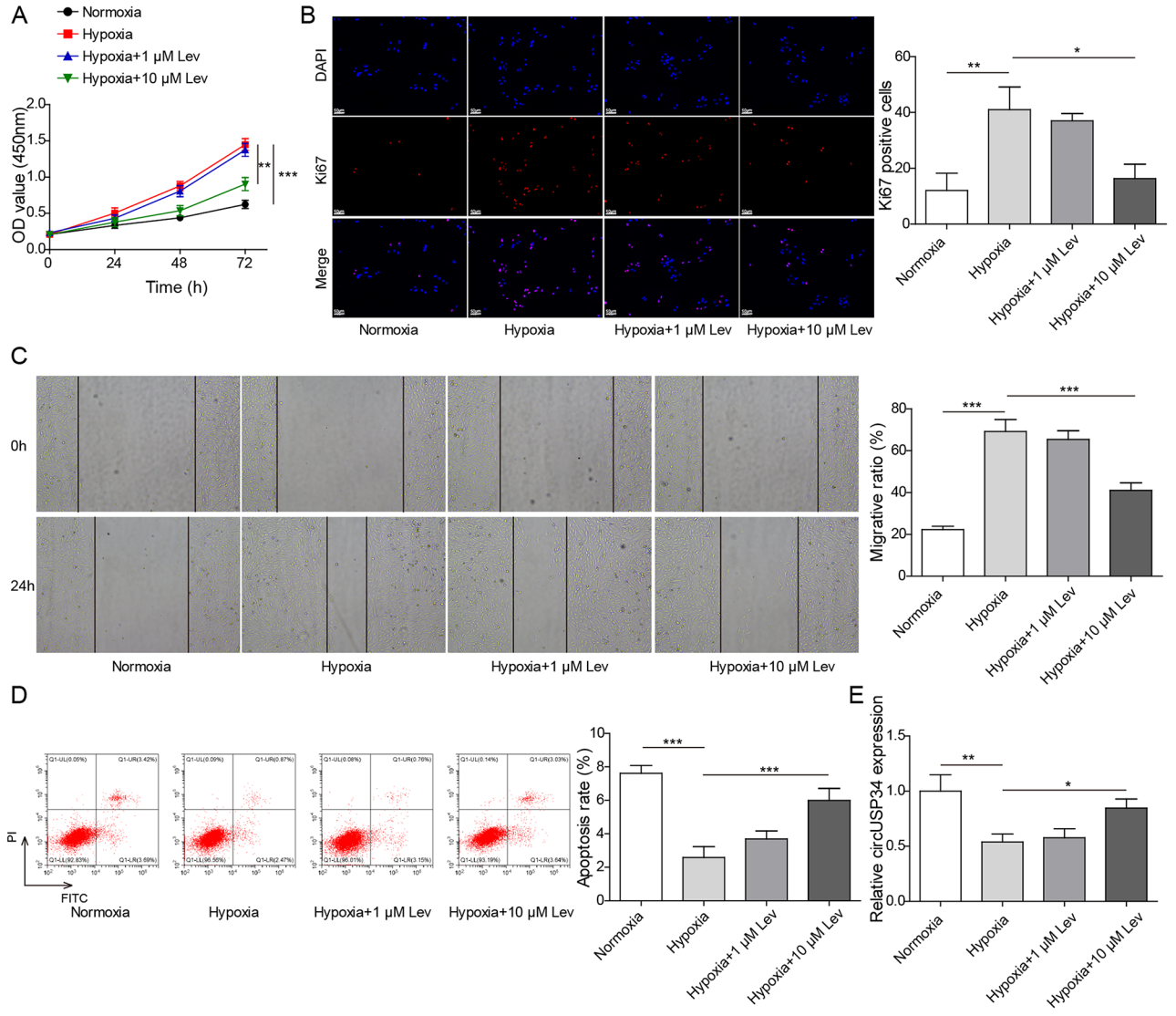

Fig. 1 Lev inhibits cell proliferation, migration and promotes apoptosis in PASMCs induced by hypoxia. **(A)** Cell proliferation was detected by CCK-8. **(B)** The expression of Ki-67 in PASMCs was examined by IF. **(C)** Cell migration ability of PASMCs was measured by cell scratch assay. **(D)** Detection of apoptosis in PASMCs by flow cytometry. **(E)** The expression of circUSP34 in PASMCs under different treatment conditions was probed by qRT-PCR assay. Data are displayed for three individual experiments with mean ± SD. *$P < 0.05$, **$P < 0.01$, ***$P < 0.001$

circUSP34 expression is dysregulated in patients with PH [13]. In our study, we examined the expression levels of circUSP34 in hypoxia-induced as well as Lev-treated PASMCs by qRT-PCR and demonstrated that hypoxia treatment significantly decreased circUSP34 expression compared with normoxia treatment, while high concentration of Lev markedly increased expression level of circUSP34 (Fig. 1E). To summarize, the results confirmed that Lev inhibited cell proliferation, migration and promoted apoptosis in hypoxia-treated PASMCs.

Lev suppresses cell proliferation, migration and facilitates apoptosis in hypoxia-treated PASMCs via upregulation of circUSP34

The results of the foregoing research found that the expression of circUSP34 was significantly decreased in hypoxia-induced PASMCs, whereas high concentration of Lev treatment substantially increased the expression level of circUSP34. To further explore whether Lev inhibits hypoxia-induced phenotype of PASMCs by modulating circUSP34, we used shRNA to knock down circUSP34 (Fig. 2A). qRT-PCR assay showed that the knockdown of circUSP34 greatly reduced the expression of circUSP34 under hypoxic conditions with Lev (Fig. 2B). CCK-8 and IF experiments show that knockdown of circUSP34 could

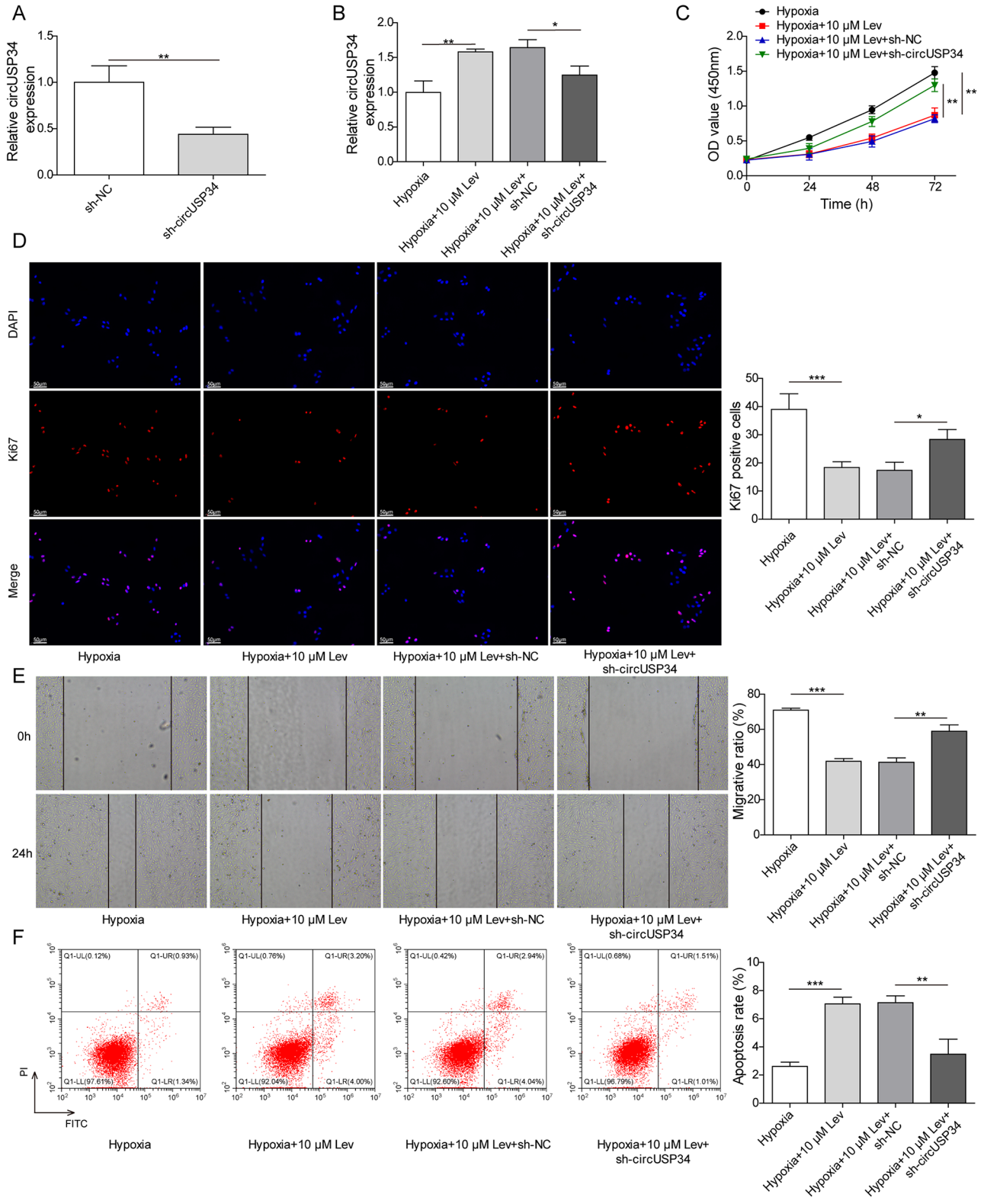

Fig. 2 Lev inhibits cell proliferation, migration and promotes apoptosis in hypoxia-treated PASMCs through upregulation of circUSP34. **(A)** qRT-PCR assay was employed to examine circUSP34 expression. **(B)** The expression of circUSP34 in PASMCs under different treatment conditions was detected by qRT-PCR assay. **(C)** Cell proliferation ability was examined by CCK-8. **(D)** Ki-67 expression in PASMCs was measured by IF. **(E)** Cell migration ability of PASMCs was assayed by cell scratch assay. **(F)** Apoptosis of PASMCs was tested by flow cytometry. Data are displayed for three individual experiments with mean ± SD. $^{*}P < 0.05$, $^{**}P < 0.01$, $^{***}P < 0.001$

notably reduce the inhibitory effect of Lev on cell proliferation of PASMCs and the expression level of Ki-67 under hypoxic conditions (Fig. 2C and D). Next, we investigated the impact of circUSP34 knockdown on cell migration capacity by performing the scratch wound assay. We discovered that the reduction of circUSP34 expression dramatically suppressed the inhibitory effect of Lev on cell migration under hypoxia conditions (Fig. 2E). Finally, the flow cytometric analysis also revealed that knockdown of circUSP34 resulted in substantial abrogation of Lev pro-apoptotic effect under hypoxic conditions (Fig. 2F). Taken together, we found that Lev inhibited cell proliferation, migration and promoted apoptosis in hypoxia-treated PASMCs via upregulation of circUSP34.

CircUSP34 regulates miR-1298 in Lev-treated and hypoxia-induced PASMCs

To study the mechanism of circUSP34 in PH regulation, we hypothesized the existence of a mutual interaction between circUSP34 and miR-1298, and predicted potential binding sites via the circular RNA interactome website [27] (Fig. 3A). Then, by a dual luciferase reporter system assay, we found that the relative luciferase activity of the experimental groups co-transfected with miR-1298 mimic and circUSP34-WT was significantly lower compared with the control group, while the relative luciferase activity of the experimental groups co-transfected with miR-1298 mimic and circUSP34-MUT had no obvious difference (Fig. 3B). The results of RIP assay indicated that circUSP34 and miR-1298 were significantly enriched in the Ago2-pulled RNA complex (Fig. 3C). Moreover, knockdown of circUSP34 with shRNA revealed a significant increase in miR-1298 expression level, while overexpression of circUSP34 resulted in a considerable suppression of miR-1298 expression level (Fig. 3D). The qRT-PCR analysis also revealed a remarkable increase in miR-1298 expression in hypoxia-treated PASMCs compared with normoxia, whilst miR-1298 expression was dramatically reduced after Lev treatment. Further knockdown of circUSP34 resulted in a significant upregulation of miR-1298 expression (Fig. 3E). To conclude, the obtained results demonstrated that circUSP34 regulates miR-1298 expression in PASMCs exposed to hypoxia and upon levosimendan treatment.

MiR-1298 regulates the expression of BMPR2

To determine the target gene of miR-1298, we used the StarBase database [28] to predict the underlying conjugation sites of miR-1298 to BMPR2 (Fig. 4A). Subsequently, we detected a significant decrease in relative

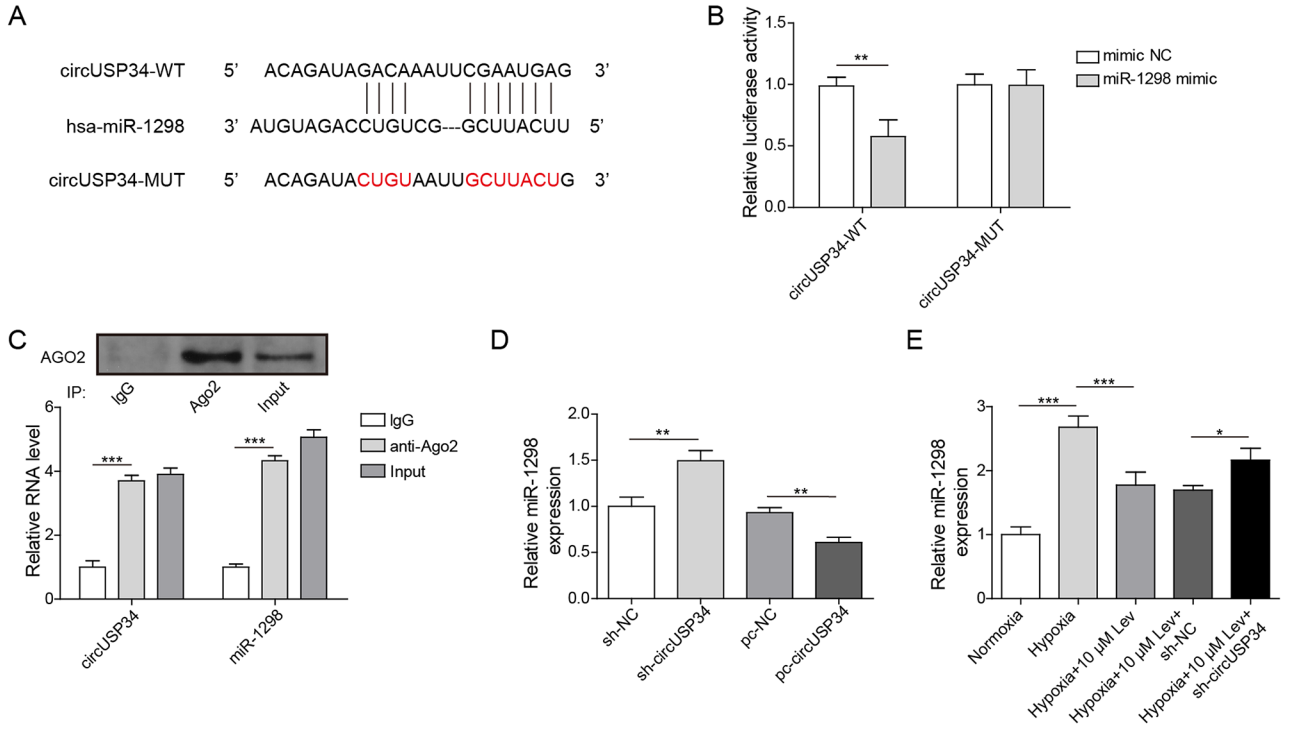

Fig. 3 CircUSP34 regulates miR-1298. **(A)** Circular RNA interactome predicted the potential binding site of circUSP34 and miR-1298. **(B)** Dual luciferase assay detected the interaction between miR-1298 and circUSP34. **(C)** RIP assay was used to test the ability of Ago2 to enrich for circUSP34 and miR-1298. **(D)** qRT-PCR assay was employed to examine miR-1298 expression in PASMCs under knockdown circUSP34 or overexpression of circUSP34. **(E)** qRT-PCR assay was applied to check miR-1298 expression in PASMCs under different treatment conditions. Data are displayed for three individual experiments with mean ± SD. *$P < 0.05$, **$P < 0.01$, ***$P < 0.001$

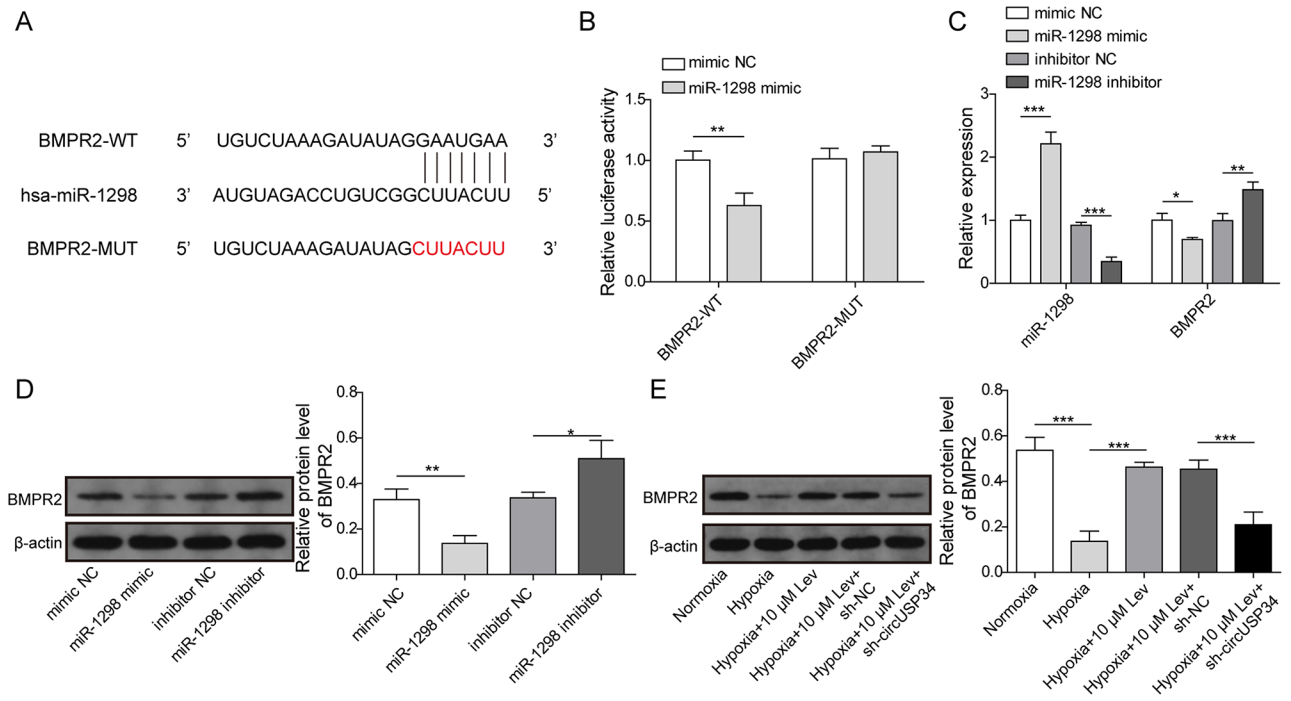

Fig. 4 BMPR2 is a target of miR-1298. **(A)** Starbase predicted the potential binding sites of miR-1298 and BMPR2. **(B)** Dual luciferase assay of miR-1298 and BMPR2 interaction. **(C)** Detection of BMPR2 expression in PASMCs after overexpression of miR-1298 or inhibition of miR-1298 by qRT-PCR assay. **(D)** WB assays were used to measure the protein expression levels of BMPR2 in PASMCs after overexpression of miR-1298 or inhibition of miR-1298. **(E)** WB assay of protein expression levels of BMPR2 in PASMCs under different treatment conditions. Data are displayed for three individual experiments with mean ± SD. $^{*}P < 0.05$, $^{**}P < 0.01$, $^{***}P < 0.001$

luciferase activity in the co-transfected miR-1298 mimic and BMPR2-WT groups compared to the control group, while the relative luciferase activity in the co-transfected miR-1298 mimic and BMPR2-MUT groups had no significant difference (Fig. 4B). Furthermore, miR-1298 expression was significantly increased and BMPR2 expression was dramatically decreased after overexpression of miR-1298, while miR-1298 expression was remarkably decreased and BMPR2 expression was markedly increased after inhibition of miR-1298 (Fig. 4C). WB analysis confirmed a remarkable decrease in BMPR2 protein expression after overexpression of miR-1298, while inhibition of miR-1298 resulted in a considerable increase in BMPR2 protein expression (Fig. 4D). Under hypoxia conditions, we found a significant decrease in BMPR2 protein level in PASMCs compared to normoxia, and treatment of hypoxic PASMCs with 10 μM levosimendan led to a remarkable increase in BMPR2 protein expression. Further knockdown of circUSP34 was followed by a dramatic decrease in BMPR2 protein expression in PASMCs treated in combination with hypoxia and drug (Fig. 4E). Consequently, the results confirm that miR-1298 inhibits BMPR2 expression in Lev-treated and hypoxia-induced PASMCs.

Lev upregulates circUSP34-targeted miR-1298-mediated BMP/Smad axis to inhibit cell proliferation, migration and promote apoptosis in hypoxia-treated PASMCs

To further confirm the effect of Lev on PH progression through regulation of circUSP34/miR-1298/BMP, rescue experiments were conducted. WB results showed a significant reduction in protein expression after knockdown of BPMR2 (Fig. 5A). Moreover, the results of WB showed that circUSP34 knockdown could inhibit the promoting effect of Lev on BMPR2 expression under hypoxia condition. In addition, inhibition of miR-1298 partially reversed the expression trend of BMPR2. And additional shRNA-mediated knockdown of BMPR2 reduced the effect of miR-1298 inhibitor (Fig. 5B). The analysis of PASMCs proliferation rate revealed that knockdown of circUSP34 significantly abolished the inhibitory effect of Lev on cell proliferation under hypoxia. Furthermore, the cell proliferation ability was partially reversed by inhibiting miR-1298. Besides, the knockdown of BMPR2 further blocked the proliferative effect of miR-1298 inhibitor (Fig. 5C). The trend of Ki-67 protein expression levels as determined by IF was consistent with the results of the determination of the proliferative capacity of PASMCs cells (Fig. 5D). Moreover, knockdown of circUSP34 markedly promoted cell migration, and inhibition of miR-1298 partially reversed this trend, while knockdown of BMPR2

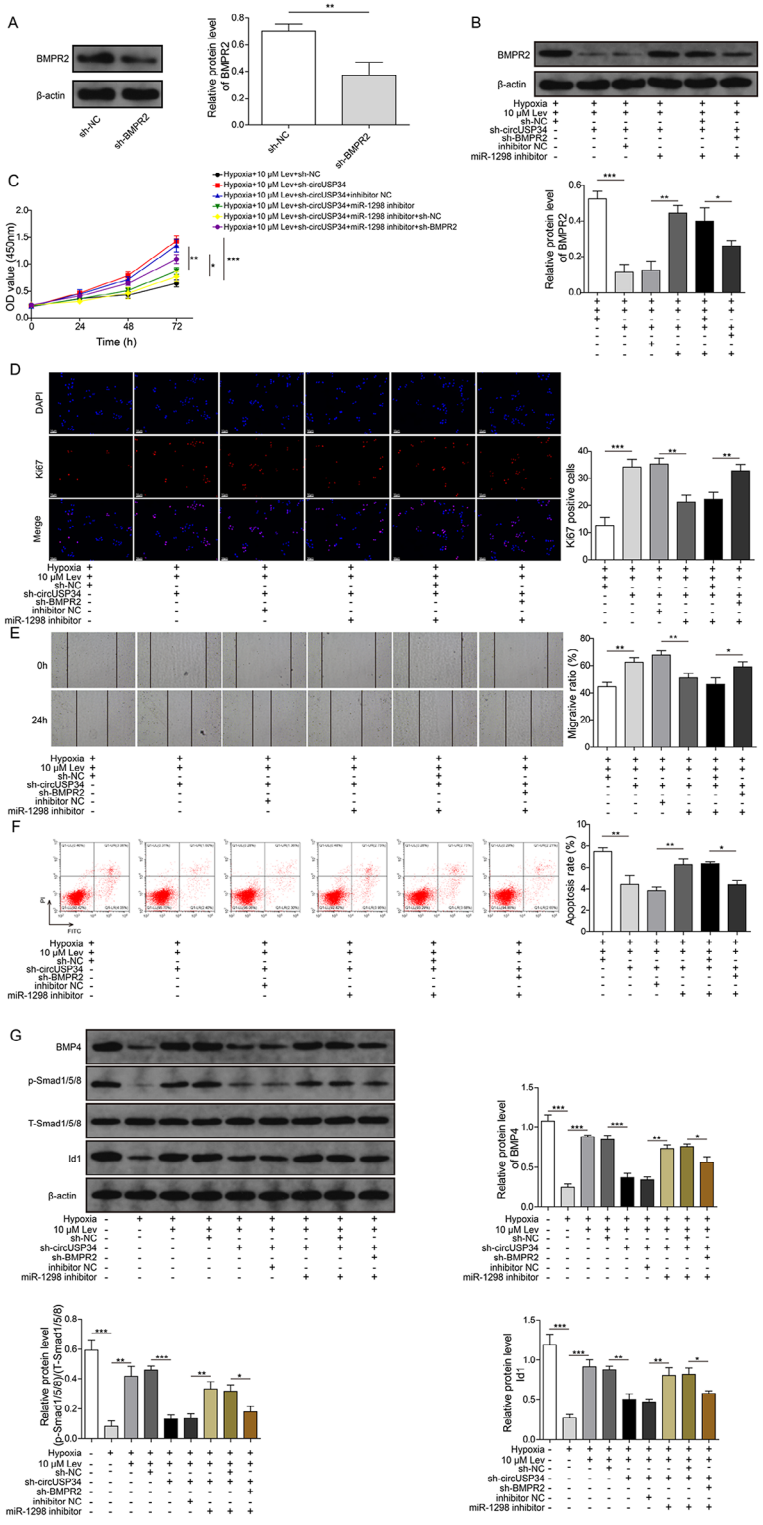

Fig. 5 Lev upregulates circUSP34-targeted miR-1298-mediated BMP/Smad axis to inhibit cell proliferation, migration and promote apoptosis in hypoxia-treated PASMCs. **(A)** The expression of BMPR2 in PASMCs was measured by WB. **(B)** The protein expression levels of BMPR2 in PASMCs under different treatment conditions were detected by WB. **(C)** The cell proliferation ability of PASMCs under different treatment conditions was examined by CCK-8. **(D)** The expression of Ki-67 in PASMCs was measured by IF. **(E)** Cell migration ability of PASMCs was tested by cell scratch assay. **(F)** Apoptosis of PASMCs was determined by flow cytometry. **(G)** WB was performed to test the protein expression levels of BMP4, p-Smad1/5/8, Id1 in PASMCs under different treatment conditions. Data are displayed for three individual experiments with mean ± SD. *$P < 0.05$, **$P < 0.01$, ***$P < 0.001$

blocked the effect of miR-1298 inhibitor on cell migration (Fig. 5E). We next examined hypoxic PASMCs apoptosis and showed that knockdown of circUSP34 significantly inhibited the promotion of apoptosis by Lev, and inhibition of miR-1298 partially reversed its trend. While further knockdown of BMPR2 reverse the effect of miR-1298 inhibitor (Fig. 5F). To further investigate the expression of BMP signaling pathways in the PH model, we examined the expression levels of BMP4, p-Smad1/5/8 and Id1, and found that BMP4, p-Smad1/5/8, and Id1 protein expression were significantly reduced after hypoxia treatment of PASMCs compared with normoxia, and when treated with Lev revealed that the expression of these proteins were restored. Hereafter, BMP4, p-Smad1/5/8, and Id1 protein expression levels were significantly reduced after knockdown of circUSP34, and inhibition of miR-1298 partially reverse their expression; while knockdown of BMPR2 was able to resist the effect of miR-1298 inhibitor (Fig. 5G). Taken together, these results suggested that Lev activates BMP/Smad signaling pathway through circUSP34-mediated miR-1298 downregulation to inhibit cell proliferation, migration and promote apoptosis in hypoxia-treated PASMCs.

Lev upregulated circUSP34-targeted miR-1298-mediated BMP/Smad axis to alleviate hypoxia combined with SU5416-induced PH

To understand the molecular mechanism of Lev treatment of PH, we induced PH in rats by hypoxia in combination with SU5416, and the RVSP, mPAP and RVI measurements showed that was successfully established a rat PH model (Fig. 6A and C). However, LVSP has not changed (Fig. 6D). In addition, HE and Masson staining results also showed significant vessel wall thickening, increased vessel wall area/total vessel area ratio in the pulmonary artery tissue and marked collagen deposition in the lung interstitial tissue in the PH group rats (Fig. 6E and F). Lev treatment was administered to the rats with PH and we found that the high dose of Lev could significantly reduce the RVSP, mPAP and RVI in the PH group rats (Fig. 6A and C), without affecting the LVSP (Fig. 6D). Besides, a high dose of Lev also reduced the ratio of vessel wall area to total vessel area in the pulmonary artery of rats (Fig. 6E) and decreased collagen deposition in the lung interstitial tissue of rats (Fig. 6F). This suggests that Lev attenuates pulmonary artery remodeling in PH rats. Similar to the cellular results, there was an increase in cell proliferation and a decrease in apoptosis in the lung tissue of PH rats. In contrast, Lev treatment clearly decreased Ki-67 expression and increased the number of TUNEL-positive cells in rat pulmonary artery tissues (Fig. 6G and H). Next, the expression of circUSP34 in pulmonary artery tissues in the rat model of PH group decreased and that of miR-1298 was increased in the model group as compared to the control group, whereas the expression of circUSP34 was increased and that of miR-1298 was decreased in the PH rats after Lev treatment. (Fig. 6I). Furthermore, the protein expression of BMPR2, BMP4, p-Smad1/5/8, Id1 was reduced in the PH rat, while the expression of BMPR2, BMP4, p-Smad1/5/8, Id1 in the PH rat after Lev treatment was obviously restored (Fig. 6J). Overall, Lev upregulated circUSP34-targeted miR-1298-mediated BMP/Smad axis to alleviate hypoxia combined with SU5416-induced PH.

Discussion

PH as a chronic disease can lead to right heart failure and death. In this regard, abnormal proliferation of pulmonary vascular cells plays a central role in PH. Previous studies have found that Lev attenuated hypoxia-induced PH [29]. High levels of Lev inhibited PDGF-induced PASMCs growth [30]. In an experimental model of PH, Lev attenuated pulmonary vascular remodeling and prevented and reversed the onset of RV failure [24]. In this study, we demonstrated that Lev not only inhibited cell proliferation, migration and promoted apoptosis in hypoxia-treated PASMCs, but also alleviated the PH phenotype induced by hypoxia combined with SU5416. The mechanism of effect was that Lev upregulated circUSP34 targeting miR-1298-mediated BMP/Smad axis to alleviate PH.

Here, our study also shown that circUSP34 is downregulated in hypoxia-induced PASMCs. When treated with Lev, circUSP34 expression was upregulated, suggesting that circUSP34 may be involved in PH progression. Recently, there is growing evidence that circRNAs are considered to be important regulators in the development of PH [9]. For example, cyclic RNA Calm4 modulates apoptosis in hypoxia-induced PASMCs via the miR-124-3p/PDCD6 axis [19]. It was shown that the circHIPK3-miR-328-3p-STAT3 axis was engaged in PAH pathogenesis through stimulation of PAEC proliferation, migration and vasculogenesis [31]. Hsa_circ_0016070 promoted proliferation and cell cycle progression of primary cultured PASMCs and regulated vascular remodeling in PH by competitively targeting miR-942-5p and increasing the expression of the downstream cell cycle protein D1 (CCND1) gene [32]. A new study was conducted to investigate a classic circRNA, CDR1, mediates the progression of vascular calcification in PH via targeted miR-7-5p [33]. Previous studies have suggested that the basic roles of circRNAs potentially consist of competing with endogenous RNAs (ceRNAs) as miRNA sponges, regulatory of gene transcription and binding of proteins, and coding for proteins [34]. Thus, we found that circUSP34 can be able to target binding and regulate miR-1298. We validated the interaction of circUSP34 and miR-1298 by dual luciferase reporter system assay and

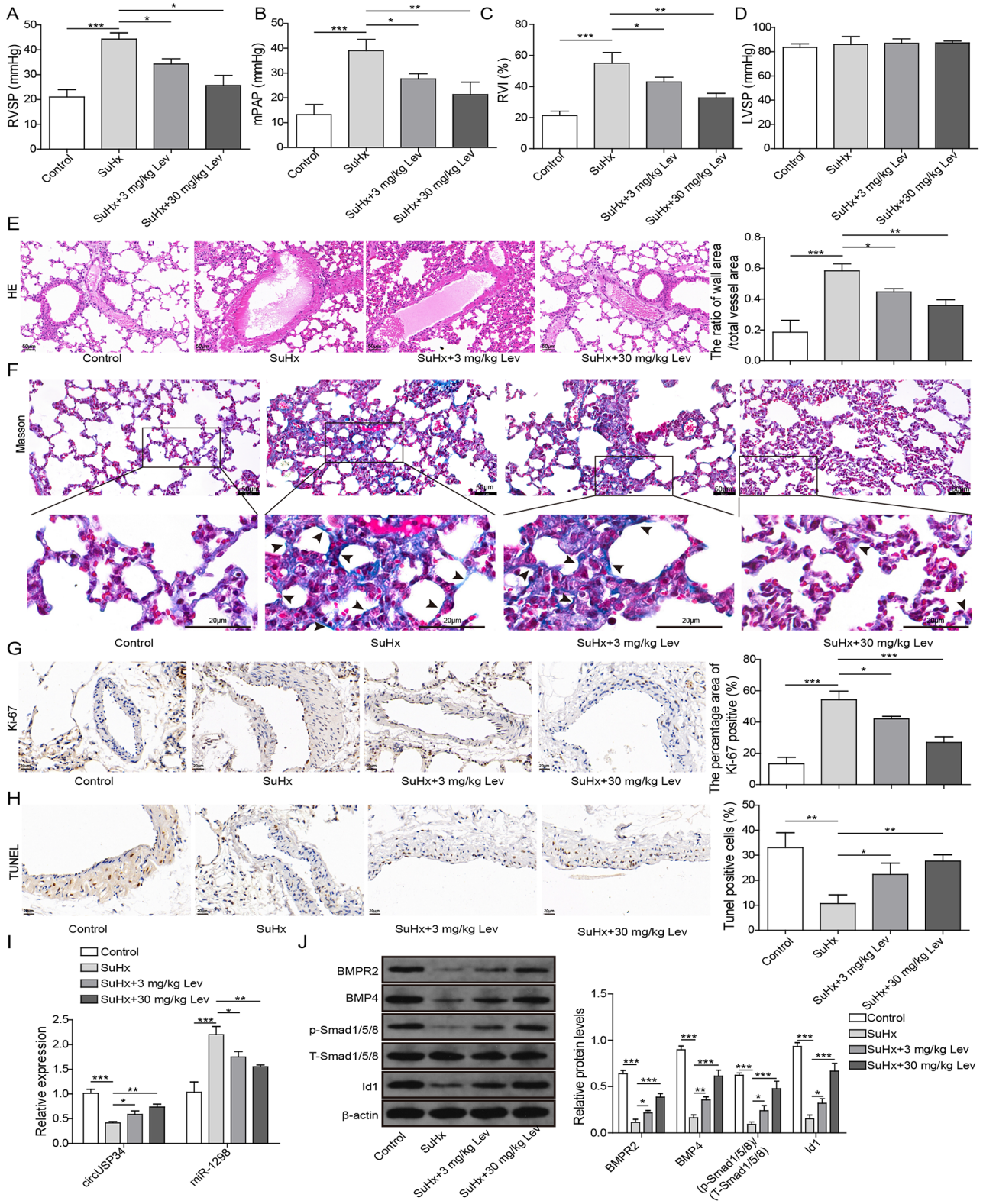

Fig. 6 Lev upregulates circUSP34-targeted miR-1298-mediated BMP/Smad axis to alleviate hypoxia combined with SU5416-induced PH. **(A)** Detection of RVSP in PH rat. **(B)** The mPAP levels were measured in PH rat. **(C)** Detection of RVI in PH rat. **(D)** Detection of LVSP in PH rat. **(E)** Examination of vascular wall changes in PH rat by HE staining. **(F)** The collagen deposition phenomenon in the lung interstitial tissue in PH rat was detected by Masson staining. **(G)** Detection of Ki-67 expression in pulmonary artery tissues in PH rat by IHC. **(H)** Apoptosis in the pulmonary artery tissue in PH rat was measured by TUNEL. **(I)** Levels of circUSP34 and miR-1298 were probed by qRT-PCR in PH rat. **(J)** WB was performed to measure the expression levels of BMPR2, BMP4, p-Smad1/5/8, and Id1 proteins in PH rat under different treatment conditions. $n = 6$, $^{*}P < 0.05$, $^{**}P < 0.01$, $^{***}P < 0.001$

RIP assay. Further knockdown of circUSP34 resulted in significant upregulation of miR-1298 expression, which also had a negative effect on dramatically suppressing the inhibitory effects of Lev on cell proliferation, migration and promotion of apoptosis under hypoxic treatment conditions.

Furthermore, we identified that miR-1298 expression was upregulated in hypoxia-treated PASMCs. When treated with Lev, the expression of circUSP34 was upregulated, whereas the expression of miR-1298 was downregulated, indicating that circUSP34 can target and regulate miR-1298. In addition, miR-1298 targets and regulates the expression of BMPR2, which affects cell proliferation, migration and apoptosis in hypoxia-treated PASMCs. Recently, a number of miRNAs have been identified as critical regulators in the progression of PH [15]. In PASMCs, the miR-130/301 family plays an invaluable function. In particular, it is involved in regulating the expression of miR-204-5p and miR-21-5p in the POU5F1/miR-130/301 family/PPARγ regulatory axis. Moreover, miR-130/301's target genes which are known in PASMCs are FOXM1, BRD4, PTEN, PSCD4, SHP2 and RUNX2, which control cell proliferation, apoptosis and differentiation [9]. Recent studies have identified miR-27a/b-3p targeting to regulate NF-κB expression involved in the upstream regulation of PPARγ in PASMCs [35]. miR-150 defended the pulmonary vasculature against pulmonary vascular remodeling and fibrosis in hypoxia-induced PH [17]. A recent study has shown that miR-1298 was upregulated in the right ventricles of PH rat compared with normal rats [18]. Thus, targeting downregulation of miR-1298 expression could assist in alleviating hypoxia-induced PH.

In summary, we demonstrated that Lev upregulated circUSP34 targeting miR-1298-mediated BMP/Smad axis to alleviate PH phenotype. Thus, the results of our study suggest that Lev can be used as a therapeutic drug for PH patients, which works through the circUSP34/miR-1298/BMP/Smad axis to alleviate PH symptoms.

Acknowledgements
Not applicable.

Author contributions
Qiang Meng and Gengxu Zhou is guarantor of integrity of the entire study. Qiang Meng contributed to the study conception and design. Linhong Song contributed to literature research. Material preparation, data collection and analysis were performed by Hui Wang and Gang Wang. The first draft of the manuscript was written by Qiang Meng and all authors commented on previous versions of the manuscript. All authors read and approved the final manuscript.

Funding
This work is supported by Research on key techniques of vital organ protection in extracorporeal life support system for children and neonatal with critical diseases (2021YFC2701704-ZGX).

Data availability
No datasets were generated or analysed during the current study.

Declarations

Ethical approval
All animal study protocols were authorized by the Animal Ethics Committee of the Seventh Medical Center of the PLA General Hospital.

Consent to participate
Not applicable.

Competing interests
The authors declare no competing interests.

Received: 15 January 2024 / Accepted: 7 August 2024
Published online: 19 August 2024

References

1. Walter K. Pulmonary hypertension. JAMA. 2021;326:1116.
2. Poch D, Mandel J. Pulmonary hypertension. Ann Intern Med. 2021;174:ltc49–64.
3. Mandras SA, Mehta HS, Vaidya A. Pulmonary hypertension: a brief guide for clinicians. Mayo Clin Proc. 2020;95:1978–88.
4. Lan NSH, Massam BD, Kulkarni SS, Lang CC. Pulmonary arterial hypertension: pathophysiology and treatment. Diseases 2018, 6.
5. Ruopp NF, Cockrill BA. Diagnosis and treatment of pulmonary arterial hypertension: a review. JAMA. 2022;327:1379–91.
6. Chen L, Wang C, Sun H, Wang J, Liang Y, Wang Y, Wong G. The bioinformatics toolbox for circRNA discovery and analysis. Brief Bioinform. 2021;22:1706–28.
7. Zhu G, Chang X, Kang Y, Zhao X, Tang X, Ma C, Fu S. CircRNA: a novel potential strategy to treat thyroid cancer (review). Int J Mol Med 2021, 48.
8. Barrett SP, Salzman J. Circular RNAs: analysis, expression and potential functions. Development. 2016;143:1838–47.
9. Zang H, Zhang Q, Li X. Non-coding RNA networks in Pulmonary Hypertension. Front Genet. 2021;12:703860.
10. Ali MK, Schimmel K, Zhao L, Chen CK, Dua K, Nicolls MR, Spiekerkoetter E. The role of circular RNAs in pulmonary hypertension. Eur Respir J 2022, 60.
11. Diao W, Liu G, Shi C, Jiang Y, Li H, Meng J, Shi Y, Chang M, Liu X. Evaluating the Effect of Circ-Sirt1 on the expression of SIRT1 and its role in Pathology of Pulmonary Hypertension. Cell Transplant. 2022;31:09636897221081479.
12. Lu GF, Geng F, Deng LP, Lin DC, Huang YZ, Lai SM, Lin YC, Gui LX, Sham JSK, Lin MJ. Reduced CircSMOC1 level promotes metabolic reprogramming via PTBP1 (polypyrimidine tract-binding protein) and mir-329-3p in pulmonary arterial hypertension rats. Hypertension. 2022;79:2465–79.
13. Miao R, Wang Y, Wan J, Leng D, Gong J, Li J, Liang Y, Zhai Z, Yang Y. Microarray expression profile of circular RNAs in chronic thromboembolic pulmonary hypertension. Med (Baltim). 2017;96:e7354.
14. Saliminejad K, Khorram Khorshid HR, Soleymani Fard S, Ghaffari SH. An overview of microRNAs: Biology, functions, therapeutics, and analysis methods. J Cell Physiol. 2019;234:5451–65.
15. Zhou G, Chen T, Raj JU. MicroRNAs in pulmonary arterial hypertension. Am J Respir Cell Mol Biol. 2015;52:139–51.
16. Chang WT, Hsu CH, Huang TL, Tsai YC, Chiang CY, Chen ZC, Shih JY. MicroRNA-21 is Associated with the severity of right ventricular dysfunction in patients with Hypoxia-Induced Pulmonary Hypertension. Acta Cardiol Sin. 2018;34:511–7.
17. Li Y, Ren W, Wang X, Yu X, Cui L, Li X, Zhang X, Shi B. MicroRNA-150 relieves vascular remodeling and fibrosis in hypoxia-induced pulmonary hypertension. Biomed Pharmacother. 2019;109:1740–9.
18. Joshi SR, Dhagia V, Gairhe S, Edwards JG, McMurtry IF, Gupte SA. MicroRNA-140 is elevated and mitofusin-1 is downregulated in the right ventricle of the Sugen5416/hypoxia/normoxia model of pulmonary arterial hypertension. Am J Physiol Heart Circ Physiol. 2016;311:H689–698.
19. Jiang Y, Liu H, Yu H, Zhou Y, Zhang J, Xin W, Li Y, He S, Ma C, Zheng X, et al. Circular RNA Calm4 regulates Hypoxia-Induced Pulmonary arterial smooth muscle cells pyroptosis via the Circ-Calm4/miR-124-3p/PDCD6 Axis. Arterioscler Thromb Vasc Biol. 2021;41:1675–93.
20. Zhang SB, Lin SY, Liu M, Liu CC, Ding HH, Sun Y, Ma C, Guo RX, Lv YY, Wu SL, et al. CircAnks1a in the spinal cord regulates hypersensitivity in a rodent model of neuropathic pain. Nat Commun. 2019;10:4119.

21. Papp Z, Agostoni P, Alvarez J, Bettex D, Bouchez S, Brito D, Černý V, Comin-Colet J, Crespo-Leiro MG, Delgado JF, et al. Levosimendan Efficacy and Safety: 20 years of SIMDAX in Clinical Use. J Cardiovasc Pharmacol. 2020;76:4–22.
22. Westphal M, Morelli A, Van Aken H. Dear levosimendan, the right ventricle will thank you! Crit Care Med. 2007;35:952–3.
23. Cholley B, Levy B, Fellahi JL, Longrois D, Amour J, Ouattara A, Mebazaa A. Levosimendan in the light of the results of the recent randomized controlled trials: an expert opinion paper. Crit Care. 2019;23:385.
24. Hansen MS, Andersen A, Holmboe S, Schultz JG, Ringgaard S, Simonsen U, Happé C, Bogaard HJ, Nielsen-Kudsk JE. Levosimendan prevents and reverts right ventricular failure in experimental pulmonary arterial hypertension. J Cardiovasc Pharmacol. 2017;70:232–8.
25. Cavusoglu Y, Beyaztas A, Birdane A, Ata N. Levosimendan and pulmonary hypertension. J Cardiovasc Med (Hagerstown). 2010;11:478–80.
26. Hansen MS, Andersen A, Nielsen-Kudsk JE. Levosimendan in pulmonary hypertension and right heart failure. Pulm Circ. 2018;8:2045894018790905.
27. Dudekula DB, Panda AC, Grammatikakis I, De S, Abdelmohsen K, Gorospe M. CircInteractome: a web tool for exploring circular RNAs and their interacting proteins and microRNAs. RNA Biol. 2016;13:34–42.
28. Li J-H, Liu S, Zhou H, Qu L-H, Yang J-H. starBase v2.0: decoding miRNA-ceRNA, miRNA-ncRNA and protein–RNA interaction networks from large-scale CLIP-Seq data. Nucleic Acids Res. 2013;42:D92–7.
29. Wiklund A, Kylhammar D, Rådegran G. Levosimendan attenuates hypoxia-induced pulmonary hypertension in a porcine model. J Cardiovasc Pharmacol. 2012;59:441–9.
30. Revermann M, Schloss M, Mieth A, Babelova A, Schröder K, Neofitidou S, Buerkl J, Kirschning T, Schermuly RT, Hofstetter C, Brandes RP. Levosimendan attenuates pulmonary vascular remodeling. Intensive Care Med. 2011;37:1368–77.
31. Hong L, Ma X, Liu J, Luo Y, Lin J, Shen Y, Zhang L. Circular RNA-HIPK3 regulates human pulmonary artery endothelial cells function and vessel growth by regulating microRNA-328-3p/STAT3 axis. Pulmonary Circulation. 2021;11:20458940211000234.
32. Zhou S, Jiang H, Li M, Wu P, Sun L, Liu Y, Zhu K, Zhang B, Sun G, Cao C, Wang R. Circular RNA hsa_circ_0016070 is Associated with Pulmonary arterial hypertension by promoting PASMC proliferation. Mol Ther Nucleic Acids. 2019;18:275–84.
33. Ma C, Gu R, Wang X, He S, Bai J, Zhang L, Zhang J, Li Q, Qu L, Xin W, et al. circRNA CDR1as promotes pulmonary artery smooth muscle cell calcification by upregulating CAMK2D and CNN3 via sponging miR-7-5p. Mol Ther Nucleic Acids. 2020;22:530–41.
34. Xu S-L, Liu J, Xu S-Y, Fan Z-Q, Deng Y-S, Wei L, Xing X-Q, Yang J. Circular RNAs Regulate Vascular Remodelling in Pulmonary Hypertension. Disease Markers 2022, 2022:4433627.
35. Xie X, Li S, Zhu Y, Liu L, Pan Y, Wang J, Shi W, Song Y, Yang L, Gao L, et al. MicroRNA-27a/b mediates endothelin-1-induced PPARγ reduction and proliferation of pulmonary artery smooth muscle cells. Cell Tissue Res. 2017;369:527–39.

Publisher's Note